This article is part of the

Proceedings of the 16th Minisymposium Verfahrenstechnik and 7th Partikelforum (TU Wien, Sept. 21/22, 2020)

Title:
Simulation Aided Pharmaceutical Hot Melt Extrusion Process Understanding, Setup and Scale-up

Corresponding author:
Josip Matic (RCPE GmbH), josip.matic@rcpe.at

Date of submission:
28.02.20

Date of revision:
10.12.20

Date of acceptance:
10.12.20

Chapter ID:
DiV2-(03)

Length:
5 pages

ISBN (full book):
978-3-903337-01-5

Simulation Aided Pharmaceutical Hot Melt Extrusion Process Understanding, Setup and Scale-up

Josip Matić[1], Johannes Khinast[1,2]
[1]Research Centre Pharmaceutical Engineering GmbH, Inffeldgasse 13/II, 8010 Graz, Austria
[2]Institute for Process and Particle Engineering, Graz University of Technology, Inffeldgasse 13/III, 8010 Graz, Austria

Keywords: Pharmaceutical HME; Product Quality; Scale-up; SPH; Mechanistic Modeling

Abstract

During the pharmaceutical product development it is important, especially in the early phases, to get a good idea about the processability of the candidate formulations. Especially for hot melt extrusion (HME) based formulations, choosing the appropriate equipment and process setup that will result in the desired product quality is not trivial. Even with small amounts of the active pharmaceutical ingredient (API) it is crucial to be able to access the processability of the formulation and possible process setups. In order to fulfil the goals mentioned above, development of formulation and process specific knowledge is required, as well as development of potent *in silico* methodologies capable of mirroring the actual process itself. This work focuses on the development of suitable *in silico* tools for the accurate HME process capturing, extended experimental investigations and product quality correlation and prediction.

Introduction

Hot melt extrusion (HME) is a continuous manufacturing process primarily using co-rotating closely intermeshing twin-screw extruders (TSE) as the equipment of choice. The process was first established in the polymer and food industries and then gradually introduced into the pharmaceutical industry, primarily as a way of increasing the solubility of purely soluble active pharmaceutical ingredients (API). The increase of API solubility is achieved by creating an amorphous solid dispersion (ASD) of the poorly soluble API by dispersing it in polymer carriers [1]–[6]. In addition to ASDs, the HME process can facilitate the creation of amorphous solid solutions and can be used as a way of controlling particle size distribution (PSD) of (nano-) crystalline APIs and imbedding them into a polymer carrier [7]–[11]. In addition to different drug delivery systems (DDS), the timing of the API release can also be controlled, resulting in DDS with immediate or controlled (extended) API release [12]–[14].

The process setup itself is extremely modular, allowing for a tailor made process for every formulation in question, with a product specific screw configuration, screw speed, throughput, barrel temperature setting, feeding points, die size and degassing pressure. However, the high process flexibility, together with the black-box nature of the process, makes choosing the appropriate process settings challenging for every new formulation and/or extruder at hand. Besides the process setup challenge, the process scale-up is a considerable issue during the different product development stages (from formulation development to pilot plant/clinical study to production scale). The current state-of-the-art is based on utilizing different extruder similarity based approaches (simple 0D models), developed mostly in the polymer industry and heavily coupled to extensive experimental efforts. The immediate restriction in the pharmaceutical industry is the lack and the expense of APIs in the early development stages in addition to the connected costs and efforts in handling the process in a GMP environment. Moreover, the 0D models do not provide any insights into the process, as they are not predictive and do not guaranty the most important aspect in the process transfer and scale-up: the equivalence of product quality at different scales [15]. Hence, understanding what role individual screw elements play in the process setup and how certain process settings lead to a certain product quality is the key for ensuring an easy process setup and a reliable subsequent process scale-up.

Materials and Methods

To respond the challenge, simulations have been increasingly used as a mean for increased process understanding. In general, HME simulations have been used for understanding individual extruder screw element pairs, the HME process as a whole and to relate HME to other unit operations in a continuous manufacturing line. The most notable among them is the investigation of individual extruder screw element pairs using the Lagrangian based Smoothed Particle Hydrodynamics (SPH) simulation approach. SPH has been used for the capturing of the melt flow and mixing phenomena in fully and/or partially filled extruder screw elements, applied for both Newtonian and non-Newtonian fluids [16]–[19]. The spatial discretization in the SPH framework is achieved by introducing moving fluid "particles", making it suitable for simulating complex moving geometries, high fluid domain deformation and free surface flow. The weakly compressible SPH method described by Monaghan [16], [20], [21] was used to discretize the Navier-Stokes equations. The discretization is done using the interpolation method, allowing the representation of a function as a set point of randomly distributed fluid "particles".

The continuity equation used is discretized as follows:

$$\frac{d\rho_a}{dt} = \sum_b m_b(\vec{v}_a - \vec{v}_b) \cdot \vec{\nabla}_a W_{ab}$$

Where m is the particle mass, $\vec{v}$ the particle velocity and $\vec{\nabla}_a W_{ab}$ is the gradient of the kernel function. The momentum equation can be discretizes as follows, including the Morris[22], [23] viscosity term and the tensile correction term $(R(f_{ab})^4)$:

$$\frac{d\vec{v}_a}{dt} = -\sum_b m_b \left(\frac{p_a}{\rho_a^2} + \frac{p_b}{\rho_b^2} + R(f_{ab})^4\right) \cdot \vec{\nabla}_a W_{ab} + \sum_b \frac{m_b(\eta_a + \eta_b)}{\rho_a \rho_b} \left(\frac{1}{|\vec{r}_{ab}|} \frac{\partial W_{ab}}{\partial r_{ab}}\right) \vec{v}_{ab} + \vec{a}$$

Where p is the particle pressure, η is the dynamic particle viscosity, $\vec{r}_{ab}$ is the distance vector between the two particles, $\vec{v}_{ab}$ is the relative particle velocity and $\vec{a}$ is a body force (i.e. gravity). The body force in the screw axis (back-pressure) is used in order to ensure different pressure states.

In order to close the system, a simplified Tait´s equation of state is used (with $\gamma = 1$):

$$p = c^2(\rho - \rho_0) + p_0$$

Where c is the speed of sound, ρ_0 the reference density

and p_0 a background pressure ensuring good particle distribution (without voids for fully filled simulations).

The speed of sound is important in order to limit the maximum allowed relative density variation, which is defined as $\delta = \Delta\rho/\rho_0$ and is mostly assumed to be $\delta = 0.01$.The speed of sound is determined in accordance to the theoretical criteria proposed by Morris:

$$c^2 \geq \frac{1}{\delta} max\left(V_0^2, \frac{\nu V_0}{L_0}, aL_0\right)$$

Where V_0 is the maximum expected fluid velocity, ν the kinematic fluid viscosity, L_0 is the relevant length scale. For predicting the required time step four time step criteria were used:

$$\Delta t \leq\leq min\left(0.25\frac{h}{c}, 0.125\frac{h^2}{\nu}, 0.25\sqrt{\frac{h}{a}}, \frac{0.3h}{c(1+1.2\alpha)}\right)$$

Where h is the smoothing length characteristic for SPH, $\alpha = 10\,\nu/hc$ is the artificial viscosity calculated from the kinematic viscosity. The first criteria is the standard Courant-Friedrich-Lewy (CLF) condition, the second and third are due to viscose and body forces respectively, and the last one takes into account the CLF and viscose limitations combined.

The kernel function used is a simple cubic-spline function, defined by the smoothing length h and the particle distance $|\vec{r}_{ab}|$:

$$W(|\vec{r}_{ab}|, h) = \frac{1}{\pi h^3}\begin{cases} 1 - \frac{3}{2}\left(\frac{|\vec{r}_{ab}|}{h}\right)^2 + \frac{3}{4}\left(\frac{|\vec{r}_{ab}|}{h}\right)^3 & 0 \leq \frac{|\vec{r}_{ab}|}{h} \leq 1 \\ \frac{1}{4}\left(2 - \frac{|\vec{r}_{ab}|}{h}\right)^3 & 1 \leq \frac{|\vec{r}_{ab}|}{h} \leq 2 \\ 0 & 2 \leq \frac{|\vec{r}_{ab}|}{h} \end{cases}$$

The smoothing length is usually set as $h = 1.2 \cdot \Delta x$, as proposed by Monaghan [16], where Δx is the particle spacing.

The results of the SPH simulation of individual screw element pairs can be represented in a dimensionless form, making it possible to rank different screw elements according to their conveying capacity, pressure build-up capacity and power consumption. Using a dimensionless representation of the results also allows for comparison and ranking of the screw pair performance at different extruder scales, allowing for a science based screw setup transfer during process scale-up. The dimensionless analysis started first with single-screw extruders [24] and was afterwards extended for twin-screw extruders [6]. The results are presented in the form of so called pressure and power characteristics of the individual screw element pairs. The pressure characteristics consist of the relation between the dimensionless throughput $(\dot{V}/nD^3)$ and the dimensionless axial pressure drop $(\Delta pD/\eta nL)$, whereas the power characteristics is a relation between the dimensionless throughput and the dimensionless driving power $(P/\eta n^2 D^2 L)$, where:

$\dot{V}$ – is the volumetric throughput;
Δp – is the pressure drop;
n – is the screw speed;
D – is the screw nominal diameter;
L – is the considered screw length;
η – is the fluid viscosity.

Theoretically and experimentally it was shown that using the correlations of the pressure and power characteristics it possible to describe the flow in fully filled, single- or twin-screw extruder elements. For the special conditions of the creeping flow regime $(Re \to 0)$, occurring in the HME process (due to high fluid viscosities), and a temperature-independent Newtonian fluid, these correlations are linear and independent of the length scale, viscosity and screw speed. The pressure and power characteristics can then be represented using the axial intercepts: A_1, A_2 and B_1, B_2:

$$\frac{\Delta pD}{\eta nL} = A_2 \cdot \left(1 - \frac{1}{A_1}\frac{\dot{V}}{nD^3}\right)$$

$$\frac{P}{\eta n^2 D^2 L} = B_2 \cdot \left(1 - \frac{1}{B_1}\frac{\dot{V}}{nD^3}\right)$$

The A_1 parameter is termed as the *inherent conveying capacity*, represents the dimensionless flow rate of a fully filled screw element when conveying without back-pressure. The B_1 is analogy the dimensionless flow rate at zero dimensionless driving power. The A_2 and B_2 parameters represent the dimensionless pressure drop and driving power respectively. These parameters are different for different screw elements and are a characteristic of the screw geometry. Knowing the dimensionless theory it is possible to describe the flow in the extruder in a simplified manner with help of a reduced order 1D HME model. This reduced order approach has the focus on understanding the process, either by investigating the melt flow in detail and/or by investigating the influence of the process settings on the process state variables like melt temperature and RTD.

The reduced order mechanistic 1D model used is the model proposed by Eitzlmayr et. all [25], [26]. Rather than representing the flow in the co-rotating twin-screw extruder as a simplified potential and shear flow, the flow is represented via mass flow rates. The geometry of the screw elements, and their ability to convey and build-up pressure, are represented by their A_1 and A_2 values. The extruder is discretized in the axial direction (x-axis), resulting in N different numerical elements. The numerical elements themselves are connected with two different types of mass flow rates. The first one account for the shear driven mass flow due to the screw geometry, and the second one accounts for the pressure driven mass flow rate due to pressure differences in the vicinity of the observed numerical element. In order to account for different types of screw elements, three numerical elements are used representing forward conveying, backward conveying and non-conveying elements. Two transition elements are used to switch between forward and backward (and vice versa) conveying elements. One additional numerical element is used to represent the die, adding up to six numerical elements types in total. The shear driven mass flow rate for forward and backward conveying elements (only the flow direction differs) for the numerical element *i* is represented as:

$$\dot{m}_{fb,i} = \rho_i K_{fb,i} n f_i A_{CR} D$$

Where f_i is the filling degree in the numerical element *i*, A_{CR} is the free cross section area and $K_{fb,i}$ is a dimensionless parameter accounting for the conveying ability of the considered screw element. The pressure driven mass flow rate is calculated for element *i* as:

$$\dot{m}_{p,i} = -\frac{D^4 \rho_i \Delta p_i}{K_{p,i}\eta_i \Delta x_i}$$

Where $K_{p,i}$ is the dimensionless parameter accounting for the flow resistance.

The dimensionless K_{fb} and K_p parameters are calculated from the A_1 and A_2 dimensionless parameters for every used screw element in the screw configuration. For actively conveying elements the parameters are calculated as:

$$K_{fb,i} = \frac{A_1 D^2}{A_{CR}}$$

$$K_{p,i} = \frac{A_2}{A_1}$$

Non-conveying elements naturally can´t be represented via A_1 and A_2 dimensionless parameters, but are represented via the slope of the pressure curve, accounting for the flow resistance as $A_0 = A_2/A_1$ for $A_1, A_2 \to 0$. Accordingly, the K_{fb} and K_p parameters for non-conveying elements are calculated as:

$$K_{fb,i} = 0$$
$$K_{p,i} = A_0$$

Combining all the mass flow rates into a mass balance equation for the observed numerical elements, taking into account the in- and outflow, it is possible to calculate the derivative of the mass content:

$$\frac{dm_i}{dt} = \rho_i A_{CR} \Delta x_i \frac{df_i}{dt} = \dot{m}_{f,i-1} + \dot{m}_{b,i+1} + \dot{m}_{p,i-1} - \dot{m}_{f,i} - \dot{m}_{b,i} - \dot{m}_{p,i}$$

Depending on the state of the numerical element observed, i.e. is it partially filled or fully filled, it is possible to calculate either the filling degree or the pressure in the observed numerical element respectively.

In addition to mass balances, energy balances are also taken into consideration. The considered heat exchange phenomena, from the side of the melt, are convection, melt-barrel and melt-screw heat transfer as well as viscose dissipation. On the side of the screw, the melt-screw heat transfer and conduction along the screw axis are taken into consideration. And on the side of the barrel, the melt-barrel heat transfer, conduction along the barrel, environmental cooling as well as external barrel heating points are taken into account.

In addition to the two simulation methods used for HME process description, the formulation being investigated has to be properly parametrized to be used as a viable input. Four main formulation properties were identified as key for the process setup: the melt viscosity, specific volume, heat capacity and thermal conductivity. The viscosity of the formulation is often represented using the Carreau-Yassuda model for non-Newtonian fluid:

$$\eta(\dot{\gamma}, T) = \frac{\eta_0 a_T}{\left(1 + \frac{|\dot{\gamma}| a_T}{\dot{\gamma}_{crit}}\right)^m}$$

Where T is the melt temperature, $\dot{\gamma}$ is the shear rate, $\dot{\gamma}_{crit}$ is the critical shear rate, η_0 the zero-shear-rate viscosity and a_T is the Williams-Landel-Ferry temperature shift factor calculated as:

$$a_T = exp\left[-\frac{C_1(T - T_r)}{C_2 + T - T_r}\right]$$

With T_r being the reference temperature. The specific volume of the formulation can be represented using the Schmidt model:

$$v_{(p,T)} = \frac{K_1}{p + K_4} + \frac{K_2 \cdot T}{p + K_3}$$

Two sets of K_1 to K_4 parameters are used, once for the solid phase (if the temperature T is below the transition temperature) and once for the liquid phase (if the temperature T is above the transition temperature). The transition temperature is a function of the pressure p, and is calculated as:

$$T_{tr(p)} = K_8 + K_9 \cdot p$$

The heat capacity and thermal conductivity are usually parametrized by using a simple linear model showing the dependency of the formulation as a function of the melt temperature.

Results

Using the two simulation approaches, together with extensive experimental efforts, it is possible to establish science based process setup and scale-up protocols. In this case, the detailed analysis of the individual screw element pairs (conveying, kneading and mixing) of two extruder sizes was performed via SPH. The two extruder sizes were chosen such to represent the formulation development (18mm size extruder) and pilot plant scale process development phase (27mm size extruder). The various screw elements were compared in regards to their pressure and power characteristics and also in regards to their distributive mixing action, Figure 1.

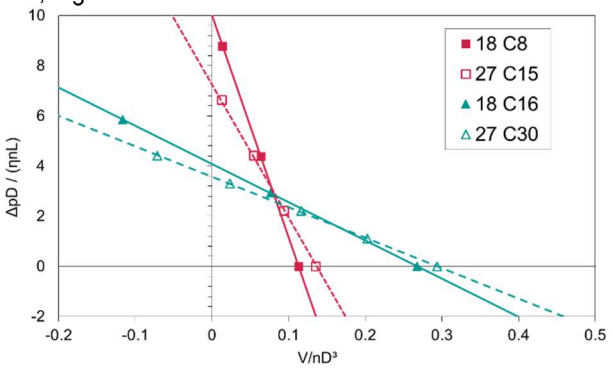

Figure 1. An example showing the performance comparison of different conveying elements screws in terms of their pressure characteristic for the two investigated extruder scales.

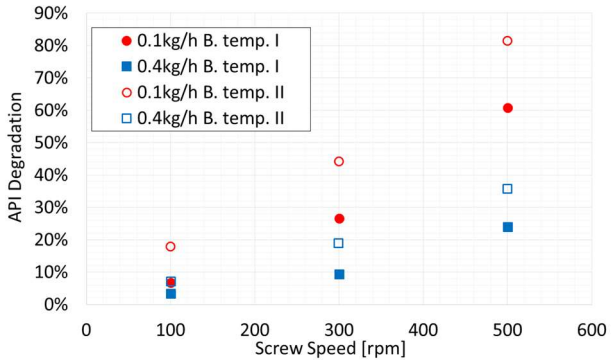

Figure 2. The DoE setup on the ZSE12 extruder showing the impact the process throughput, screw speed and barrel temperature have on the API degradation in the final extrudate.[27]

Following the SPH study, various DoE settings on the smaller 12mm extruder were performed with the goal of understanding the resulting API degradation, and connecting it with the process settings and resulting process state, Figure 2. The results of the API degradation were carefully analyzed and correlations were established showing the API degradation as a function of the used independent process variables, like screw speed, throughput and barrel temperature. In addition to the correlations to the independent process variables, the dependent process variables like the specific mechanical energy consumption (SMEC) and the residence time distribution (RTD) were also investigated and correlations with the API degradation were established, Figure 3 and Figure 4.

It was found that neither the independent nor dependent process variables are uniquely suited to ambiguously indicate the level of API degradation expected in the product. As a response, detailed 1D HME simulations of the various HME process states were performed and analyzed, showing the axially resolved (in the direction of the screw) values of the melt temperature, SMEC, filling degree, pressure distribution and local RTD. This additional information helped to make the process more transparent and allowed to establish a unique relation between the API degradation and the internal process state that resulted out of the chosen process settings.

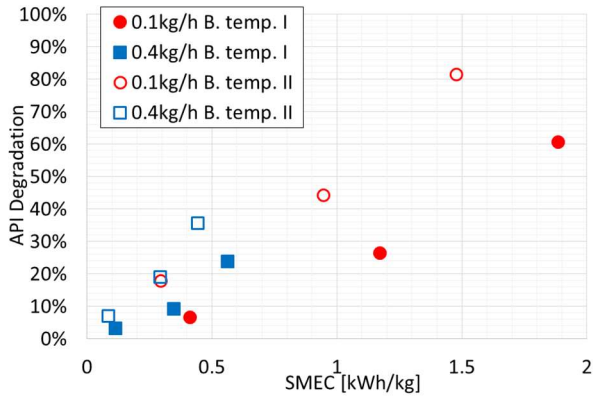

Figure 3. Influence of the SMEC on the API degradation in the final extrudate. [27]

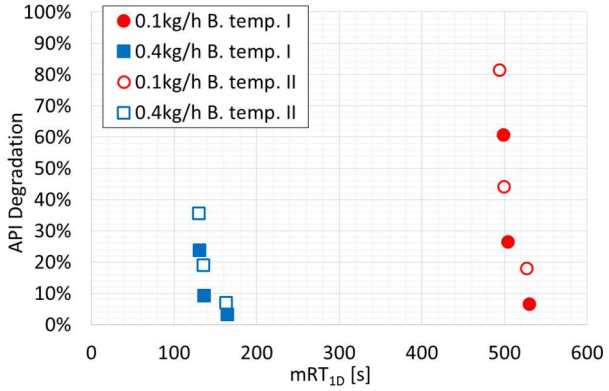

Figure 4. Influence of the mean residence time on the API degradation in the final extrudate. [27]

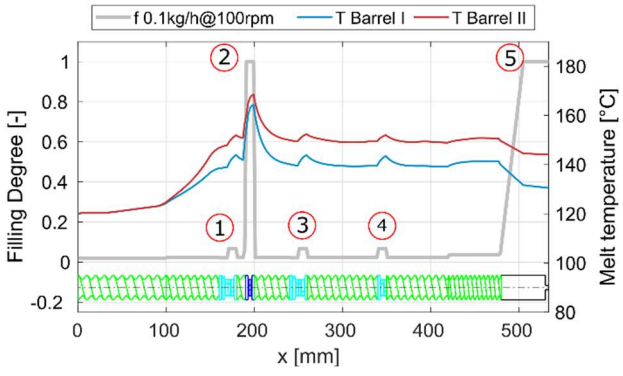

Figure 5. An example of the 1D HME simulation results showing the filling degree and melt temperature for one process setting (0.1kg/h at 100rpm) and two barrel temperatures, on the ZSE12 extruder. [27]

As HME process scale-up is still a significant challenge, the decision was made to test the different scale-up approaches that can be found in the literature. It was decided to test six different scale-up approaches with additional nine DoE settings on the 18mm pilot plant size extruder. The screw transfer was performed using the previously characterized screw element pairs. The analysis of the product quality was done similar to the study done on the smaller 12mm extruder, i.e. the API degradation was analyzed as a function of various independent and dependent variables with the goal of establishing direct correlations. At the end, using the 1D HME simulations it was possible to directly connect the API degradation results with the internal state of the process, increasing the certitude that *in silico* tool can be used as a means for science based HME process setup and scale-up.

Conclusion

Based on the knowledge gained from extensive and systematic HME processing experiments; detailed screw element pair and whole process simulations, and product quality investigations, it is clear that knowing only the dependent and independent HME process variables in not enough to guaranty the desired product quality as an outcome of the process. Using the different *in silico* tools, in combination with traditional approaches, helps in making the HME process more approachable and in moving away from a black box process. Understanding the process state certain process settings produce helped in directly correlating the achieved API degradation to the melt temperatures and local RTD in the HME process.

Outlook

The next challenge is the development of tools for the *in silico* prediction of the product performance, i.e. not only correlating the product quality with the process state, but actively predicting the product quality out of the prevailing process state before any extrusion experiments are performed. Apart from relating the process state to the product quality, as done in this study, it is important to develop simple, extrusion like, early formulation screening tools for establishing formulation process maps. Such maps would then be used to specify the limits of the process states can reach, and via *in silico* tools like SPH and 1D HME, it would then be possible to perform process setup and scale-up purely *in silico*, before any actual extrusion experiments were yet performed. This would further significantly reduce the cost and risk of pharmaceutical product development via the HME continuous manufacturing route, and greatly reduce the time to market of such pharmaceutical products.

References

[1] K. Kolter, M. Karl, and A. Gryczke, *Hot-Melt Extrusion with BASF polymers*, no. 2nd Revised and Enlarged. BASF, 2012.

[2] H. McFall *et al.*, “Formulation of aripiprazole-loaded pH-modulated solid dispersions via hot-melt extrusion technology: In vitro and in vivo studies,” *Int. J. Pharm.*, vol. 554, pp. 302–311, Jan. 2019.

[3] J. M. Vasoya *et al.*, “Development of Solid Dispersion by Hot Melt Extrusion Using Mixtures of Polyoxylglycerides With Polymers as Carriers for Increasing Dissolution Rate of a Poorly Soluble Drug Model,” *J. Pharm. Sci.*, vol. 108, no. 2, pp. 888–896, Feb. 2019.

[4] A. Schittny, H. Ogawa, J. Huwyler, and M. Puchkov, “A combined mathematical model linking the formation of amorphous solid dispersions with hot-melt-extrusion process parameters,” *Eur. J. Pharm. Biopharm.*, vol. 132, pp. 127–145, Nov. 2018.

[5] H. Patil, R. V. Tiwari, and M. A. Repka, “Hot-Melt Extrusion: from Theory to Application in Pharmaceutical Formulation,” *AAPS PharmSciTech*, vol. 17, no. 1, pp. 20–42, Feb. 2016.

[6] K. Kohlgrüber, *Co-Rotating Twin-Screw Extruder*. München: Carl Hanser Verlag GmbH & Co. KG, 2007.

[7] R. Baumgartner, A. Eitzlmayr, N. Matsko, C. Tetyczka, J. G. Khinast, and E. Roblegg, “Nano-

extrusion: A promising tool for continuous manufacturing of solid nano-formulations," *Int. J. Pharm.*, vol. 477, no. 1–2, pp. 1–11, Dec. 2014.

[8] R. Baumgartner, J. Matić, S. Schrank, S. Laske, J. Khinast, and E. Roblegg, "NANEX: Process design and optimization," *Int. J. Pharm.*, vol. 506, no. 1–2, pp. 35–45, Jun. 2016.

[9] A. M. Bhagurkar, M. A. Repka, and S. N. Murthy, "A Novel Approach for the Development of a Nanostructured Lipid Carrier Formulation by Hot-Melt Extrusion Technology," *J. Pharm. Sci.*, vol. 106, no. 4, pp. 1085–1091, Apr. 2017.

[10] L. A. D. Silva *et al.*, "Preparation of a solid self-microemulsifying drug delivery system by hot-melt extrusion," *Int. J. Pharm.*, vol. 541, no. 1–2, pp. 1–10, Apr. 2018.

[11] H. Patil, X. Feng, X. Ye, S. Majumdar, and M. A. Repka, "Continuous Production of Fenofibrate Solid Lipid Nanoparticles by Hot-Melt Extrusion Technology: a Systematic Study Based on a Quality by Design Approach," *AAPS J.*, vol. 17, no. 1, pp. 194–205, Jan. 2015.

[12] Y. Zhu, N. H. Shah, A. Waseem Malick, M. H. Infeld, and J. W. McGinity, "Controlled Release of a Poorly Water-Soluble Drug from Hot-Melt Extrudates Containing Acrylic Polymers," *Drug Dev. Ind. Pharm.*, vol. 32, no. 5, pp. 569–583, Jan. 2006.

[13] A. Q. Vo *et al.*, "A novel floating controlled release drug delivery system prepared by hot-melt extrusion," *Eur. J. Pharm. Biopharm.*, vol. 98, pp. 108–121, Jan. 2016.

[14] M. Fukuda, N. A. Peppas, and J. W. McGinity, "Floating hot-melt extruded tablets for gastroretentive controlled drug release system," *J. Control. Release*, vol. 115, no. 2, pp. 121–129, Oct. 2006.

[15] J. Matić, A. Witschnigg, M. Zagler, S. Eder, and J. Khinast, "A novel in silico scale-up approach for hot melt extrusion processes," *Chem. Eng. Sci.*, vol. 204, pp. 257–269, Aug. 2019.

[16] J. J. Monaghan, "Smoothed particle hydrodynamics," *Reports Prog. Phys.*, vol. 68, no. 8, pp. 1703–1759, Aug. 2005.

[17] K. Kohlgrüber and W. Wiedmann, *Co-Rotating Twin-Screw Extruders*. Munich: Carl Hanser Verlag, 2008.

[18] A. Eitzlmayr and J. G. Khinast, "Co-rotating twin-screw extruders: Detailed analysis of conveying elements based on smoothed particle hydrodynamics. Part 1: Hydrodynamics," *Chem. Eng. Sci.*, vol. 134, pp. 861–879, Sep. 2015.

[19] A. Eitzlmayr, J. Matić, and J. G. Khinast, "Analysis of flow and mixing in screw elements of corotating twin-screw extruders via SPH," *AIChE J.*, vol. 63, no. 6, pp. 2451–2463, Jun. 2017.

[20] R. A. Gingold and J. J. Monaghan, "Smoothed particle hydrodynamics: theory and application to non-spherical stars," *Mon. Not. R. Astron. Soc.*, vol. 181, no. 3, pp. 375–389, Dec. 1977.

[21] J. J. Monaghan, "Smoothed Particle Hydrodynamics," *Annu. Rev. Astron. Astrophys.*, vol. 30, pp. 543–574, 1992.

[22] J. ~.- Morris and P. ~J. Fox, "Modeling low Reynolds number incompressible flows using SPH," *J. Comput. Phys.*, vol. 136, no. 136, pp. 214–226, 1997.

[23] J. P. Morris, "A Study of the Stability Properties of SPH," *Monash Appl. Math. Reports Prepr.*, p. 4, 1995.

[24] J. Pawlowski, *Die Ähnlichkeitstheorie in der physikalisch-technischen Forschung*. Berlin, Heidelberg: Springer Berlin Heidelberg, 1971.

[25] A. Eitzlmayr *et al.*, "Experimental characterization and modeling of twin-screw extruder elements for pharmaceutical hot melt extrusion," *AIChE J.*, vol. 59, no. 11, pp. 4440–4450, Nov. 2013.

[26] A. Eitzlmayr *et al.*, "Mechanistic modeling of modular co-rotating twin-screw extruders," *Int. J. Pharm.*, vol. 474, no. 1–2, pp. 157–176, Oct. 2014.

[27] J. Matić *et al.*, "Towards predicting the product quality in hot-melt extrusion: Small scale extrusion," *Int. J. Pharm. X*, vol. 2, p. 100062, Dec. 2020.